


# Comparative Study of Two Common *In Vitro* Models for the Pancreatic Islet with MIN6

Xinxin Chao<sup>1,5</sup> · Furong Zhao<sup>1,6</sup> · Jiawei Hu<sup>1,2</sup> · Yanrong Yu<sup>3</sup> · Renjian Xie<sup>1,2</sup> · Jianing Zhong<sup>1,2</sup> · Miao Huang<sup>1,2</sup> · Tai Zeng<sup>1,2</sup> · Hui Yang<sup>1,2</sup>  · Dan Luo<sup>4</sup> · Weijie Peng<sup>1,2,3</sup>

Received: 20 October 2022 / Revised: 20 October 2022 / Accepted: 30 October 2022 / Published online: 2 January 2023  
© Korean Tissue Engineering and Regenerative Medicine Society 2022

## Abstract

**BACKGROUND:** Islet transplantation is currently considered the most promising method for treating insulin-dependent diabetes. The two most-studied artificial islets are alginate-encapsulated  $\beta$  cells or  $\beta$  cell spheroids. As three-dimensional (3D) models, both artificial islets have better insulin secretory functions and transplantation efficiencies than cells in two-dimensional (2D) monolayer culture. However, the effects of these two methods have not been compared yet. Therefore, in this study, cells from the mouse islet  $\beta$  cell line Min6 were constructed as scaffold-free spheroids or alginate-encapsulated dispersed cells.

**METHODS:** MIN6 cell spheroids were prepared by using Agarose-base microwell arrays. The insulin secretion level was determined by mouse insulin ELISA kit, and the gene and protein expression status of the MIN6 were performed by Quantitative polymerase chain reaction and immunoblot, respectively.

**RESULTS:** Both 3D cultures effectively promoted the proliferation and glucose-stimulated insulin release (GSIS) of MIN6 cells compared to 2D adherent cells. Furthermore, 1% alginate-encapsulated MIN6 cells demonstrated more significant effects than the spheroids. In general, three pancreatic genes were expressed at higher levels in response to the 3D culture than to the 2D culture, and pancreatic/duodenal homeobox-1 (PDX1) expression was higher in the cells encapsulated in 1% alginate than that in the spheroids. A western blot analysis showed that 1% alginate-encapsulated MIN6 cells activated the phosphoinositide 3-kinase (PI3K)/serine/threonine protein kinase (AKT)/forkhead transcription factor FOXO1 (FoxO1) pathway more than the spheroids, 0.5% alginate-, or 2% alginate-encapsulated cells did. The 3D MIN6 culture, therefore, showed improved effects compared to the 2D culture, and the 1% alginate-encapsulated MIN6 cells exhibited better effects than the spheroids. The upregulation of PDX1 expression through the activation of the PI3K/AKT/FoxO1 pathway may mediate the improved cell proliferation and GSIS in 1% alginate-encapsulated MIN6 cells.

**CONCLUSION:** This study may contribute to the construction of *in vitro* culture systems for pancreatic islets to meet clinical requirements.

**Keywords** MIN6 · Cell spheroid · PI3K/AKT/FoxO1

Xinxin Chao, Furong Zhao, Jiawei Hu. co-first authors.

✉ Hui Yang  
yanghui\_2521@gmu.edu.cn

✉ Dan Luo  
thinker\_20080502@126.com

✉ Weijie Peng  
pengweijie@gmu.edu.cn

<sup>1</sup> Jiangxi Provincial Key Laboratory of Biomaterials and Biofabrication for Tissue Engineering, Gannan Medical University, Ganzhou, China

<sup>2</sup> Key Laboratory of Prevention and Treatment of Cardiovascular and Cerebrovascular Diseases, Ministry of Education, Gannan Medical University, Ganzhou, China

## 1 Introduction

Type 1 diabetes damages the  $\beta$  cells in the pancreatic islet due to autoimmune causes, which suppress the insulin secretion function and increase blood glucose levels [1–4]. The requirement for lifelong insulin injections to treat Type 1 diabetes has motivated researchers to explore the efficiency of islet transplantation [5, 6]. A popular method of islet transplantation, known as the Edmonton Protocol, has been used since 2000. Its low invasive damage, stable efficacy, and minimal side effects has made it a promising long-term cell therapy method and the first choice for current cell therapies [7, 8]. This method allows 85% of recipients to be off insulin for at least 1 year as cadaveric pancreatic cells are harvested and infused into the portal vein [9]. However, due to the scarcity of pancreatic donors and long-term anti-immunotherapy, its application remains limited [10], and the utilization of alternative cells to fabricate artificial islet for transplantation has become a new hotspot in this field. Currently, several alternative cell sources for  $\beta$  cells are being explored, with the emergence of various approaches for developing artificial islets using tissue engineering, including scaffold-based bioengineering, macro-devices, insulin-secreting organoids, three-dimensional (3D) bioprinting, and pancreas-on-chip. Two tissue-engineering artificial islet transplantation methods have been mainly studied: one involves transplanting the encapsulated insulin-secreting cells into a hydrogel, and the other involves transplanting insulin-secreting cell aggregates or spheroids [9–15].

The encapsulation of insulin-secreting cell into a hydrogel is to involves encapsulating the islets or  $\beta$ -like cells in semi-permeable hydrogel that would enable the transportation of nutrients, sugars and insulin substances, but would prevent immunoglobulins, complementary cells, and immune cells, which would avoid the need for immunosuppressive agents. Sodium alginate is the most used hydrogel material [16]. Alginate encapsulation is often performed using a digested single-cell suspension

mixed with alginate solution [17]. The sizes of the islets are important to assess and ensure successful islet transplantations [18]. The transplantation of larger islets is often less effective due to hypoxic necrosis in the core [19]. Because endovascular grafts, such as portal vein perfusion, may induce thrombosis, alginate-encapsulated bodies are generally transplanted extravascularly, including subcutaneously, in the renal capsule, or greater omentum. This method has long been reported in clinical studies [20].

Insulin-secreting cell aggregates or spheroids involve proliferation and aggregation of  $\beta$ -like cells *in vitro*. The limited sources of human primary islet cells has encouraged the analysis of other cell sources, including islet cell lines such as MIN6 [21], human embryonic stem cells [17, 22], islet stem cells [23], human induced pluripotent stem cells [24, 25], and islet-secreting cells arising from transdifferentiation of other cells such as  $\alpha$ -cells [26] and hepatocytes [27]. Intra-islet cellular interactions help maintain islet function and contribute to the development and maintenance of the  $\beta$  cell phenotype and upregulation of insulin gene expression [28]. Disseminated  $\beta$  cells form pseudo-islets after repolymerization and can increase cell viability and glucagon release levels in a manner similar to that of native  $\beta$  cells [29]. Therefore, insulin-secreting cells must form spheroids before transplantation. In clinical practice, islet transplantation is usually performed by injecting islets into hepatic sinusoids through the portal vein. Islet tissues may also be embedded into the kidney sac or omentum, as demonstrated in previous animal studies [30].

Differences in the microenvironment can affect cell behavior and function [31]. Conventional two-dimensional (2D) monolayer culture is currently the most widely used method [32]. However, due to the scarcity of cell–cell and cell–matrix interactions, 2D culture cannot effectively represent the physiological properties of cells [33]. Recently, the development and application of three-dimensional (3D) culture systems have received extensive attention [34]. Owing to their potential to simulate cell–cell and cell–matrix interactions and provide the physical stimulators required for cell growth and differentiation, 3D culture systems are considered to be more representative of *in vivo* physiological properties [35, 36]. Three-dimensional culture systems may be classified as scaffold-based or scaffold-free depending on the presence of scaffold materials [37, 38]. Alginate encapsulated artificial islets and islet cell spheroids are scaffold-based or scaffold-free cultured 3D tissue-engineered islets, respectively. Numerous *in vitro* and *in vivo* experiments have shown that artificial islets cultured using both methods perform significantly better than those in 2D monolayer cultures. Insulin secretion and glucose-stimulated insulin release (GSIS) levels in alginate-encapsulated insulin-secreting

<sup>3</sup> Jiangxi Provincial Key Laboratory of Basic Pharmacology, School of Pharmaceutical Science, Nanchang University, Nanchang, China

<sup>4</sup> Department of Physiology, School of Basic Medicine, Nanchang University, Nanchang, China

<sup>5</sup> The Affiliated Hospital of Jining Medical University, Shandong, China

<sup>6</sup> Department of Clinical Pharmacy, The First Affiliated Hospital of Shandong First Medical University & Shandong Provincial Qianfoshan Hospital, Shandong, China

cells have been found to be significantly higher than those in 2D monolayer cultures [10]. Additionally, dispersed human islet cells may be used to construct spheroids. Studies involving the transplantation of spheroids into diabetic mouse models have demonstrated that the glucose metabolism levels are similar to those following the transplantation of natural islets, while the transplantation of 2D cells did not significantly improve the glucose metabolism levels [29, 30].

Although both 3D cultured tissue-engineered islets have better insulin secretory function and GSIS levels, they have only been compared with 2D cultured cells. To date, the effects of these two methods have not been directly compared. By comparing the effects of the two methods and exploring their underlying mechanisms, the factors influencing tissue-engineered islet transplantation can be used to optimize the construction method and transplantation conditions used. Therefore, this study compared the functional differences between the two 3D-tissue-engineered islets to analyze their underlying mechanisms.

Islet  $\beta$  cells are located in the islets that are distributed throughout the pancreas and account for only 1% of the total volume of the pancreas. It is relatively difficult to isolate a large number of primary islets and because the islets contain mostly other cells rather than  $\beta$  cells. In this study, MIN6 cells, which are mouse islet tumor cells with insulin-secreting ability, were used instead of animal pancreatic tissues to isolate islet cells. The insulin secretion pattern of MIN6 cells in spheroid culture is similar to that of isolated human or mouse islets, which are often used as PI models to simulate islet function [39]. Therefore, in this study, monolayer-cultured MIN6 cells were used as a control to compare cell spheroids and dispersed cells encapsulated in alginate gel. The changes in insulin secretion function and its underlying mechanisms under different culture methods of MIN6 were also observed to provide a basis for the analysis of the two islet cell transplantation methods.

## 2 Materials and methods

### 2.1 Materials

All reagents used in this study were purchased from Sigma Chemical Co. (St. Louis, MO, USA) except otherwise stated. The mouse pancreatic  $\beta$  cell line MIN6 was obtained from Fu Heng Cell Center (NO. FH0390, Shanghai, China). The RPMI 1640 medium, FBS and CellTiter-Glo<sup>®</sup> 3D reagents were purchased from Invitrogen (Thermo Fisher Scientific Inc., Waltham, MA, USA). The deionized water was obtained by using a water purification system (Millipore S.A.S., Guyancourt, France).

The primary antibodies and secondary antibodies were purchased from Abcam, Cambridge, UK. The chemiluminescence kit and calcein/propidium iodide were obtained from Bio-Rad (Hercules, CA, USA). The mouse insulin ELISA kit was supplied by Cloud-clone (CEA448Mu, Wuhan, China). All other reagents were of analytical grade.

### 2.2 Cell culture

The mouse pancreatic  $\beta$  cell line MIN6 was cultured in RPMI 1640 medium supplemented with 10% fetal bovine serum (FBS), 100  $\mu\text{g}/\text{mL}$  streptomycin, 100 U/mL penicillin, 10 mmol/L HEPES and 50  $\mu\text{mol}/\text{L}$   $\beta$ -mercaptoethanol at 37 °C in a humidified environment with 5%  $\text{CO}_2$ . The cells were passaged with trypsin (0.5% v/v) every 3 days.

### 2.3 Preparation of MIN6 spheroids

Agarose-base microwell arrays with a diameter and depth of 400  $\mu\text{m}$  are constructed using replica molding with 3D printing technology (Envision, Hamburg, Germany). The trypsin-digested cell suspension (300  $\mu\text{L}$ ) was added to a 12-well plate loaded with microwell array molds. The cell density was approximately  $3 \times 10^5$  cells/well. The cells were incubated for 2 h, and 700  $\mu\text{L}$  of fresh complete medium were added after most of the cells had settled and aggregated. The fluid was changed every other day. After 1 days of incubation, uniform cell spheroids were observed in the microporous.

### 2.4 Preparation of alginate microbeads encapsulated MIN6 cells

Sodium alginate powder was treated with UV light for 4 h; a mass of sodium alginate powder was dissolved in sterile deionized water and stirred for 3 h to form clarified colloids with concentrations of 0.5%, 1% and 2%(w/v). The cell suspension was mixed with sodium alginate colloid at a volume ratio of 1:1 to obtain a final concentration of  $1 \times 10^6$  cells/mL. After blowing well, the mixture was added dropwise into a sterile calcium chloride solution (100 mM) using a syringe (needle type 25G). The medium was washed three times and removed; after which complete medium was added for further cultivation.

### 2.5 Cell viability and proliferation analysis of different concentrations of hydrogel encapsulation

We selected final concentrations of 0.5%, 1% and 2% (w/v) of alginate-encapsulated cells for 3D culture. Cell viability was tested using the standard operating procedure of the

live-dead staining kit. The cells were cultured under different conditions for 5 days and stained using calcein/propidium iodide (AM/PI), and incubated with the cells for 30 min before being observed using a confocal laser scanning microscope (ZEISS 880; Zeiss, Oberkochen, Germany). The CellTiter-Glo<sup>®</sup> 3D reagent was then used to detect the proliferation behavior of cells under different culture conditions. The starting cell density was maintained consistently and cultured until Days 3, 5, and 7, after which an equal volume of the working solution was added to the medium. The cells were incubated for 30 min at 25 °C and then left for 30 min to fully lyse the cells. Afterwards, 100 µL of reaction solution from each well was transferred to a white-walled 96-well plate, and the proliferation level was measured using a multifunctional enzyme marker (PerkinElmer, Waltham, MA, USA). Cellular ATP levels were standardized using the Bradford protein quantification assay.

## 2.6 Imaging by scanning electron microscopy

The cell spheroids and alginate microbeads were fixed with precooled paraformaldehyde at 4 °C and dehydrated with 40%, 60%, 80% and 100% ethanol. The collected cell spheroids were placed on the platform, and the alginate microbeads were gently cut using a sharp blade. The cut side was placed on the platform for gold spraying and imaging using scanning electron microscopy (SEM, Sigma, Zeiss).

## 2.7 Cell viability and proliferation analysis under different culture conditions

MIN6 cells were cultured under different conditions for 3, 5 and 7 days. The cells in the various culture environments were stained using AM/PI for 30 min before being observed using a confocal laser scanning microscope (ZEISS 880, Zeiss). The cellTiter-Glo<sup>®</sup> 3D reagent was used to detect the proliferation of the cells under different culture conditions. Cellular ATP level was standardized by the Bradford protein quantification assay.

## 2.8 Quantitative analysis of insulin secretion

Insulin secretion measurements were performed using glucose stimulated insulin secretion (GSIS). The initial cell density was maintained at the same level. After 5 days of incubation, the medium was removed, and Krebs–Ringer bicarbonate HEPES buffer (KRBH) was added and incubated for 30 min. The glucose-free medium was washed and incubated for 90 min with stimulatory glucose (25.5 mM) and low glucose (5.5 mM) media, and the supernatant was collected. Insulin secretion levels were

measured by mouse insulin ELISA kit and standardized using the Bradford protein quantification assay. The glucose stimulation index (GSI) was calculated by dividing the insulin secretion at 25.5 mM by the insulin secretion at 5.5 mM glucose.

## 2.9 Quantitative real-time PCR analysis

After extraction of cellular RNA, the concentration and purity of RNA were measured using ultra-micro spectrophotometer (ABI, Valencia, CA, USA). cDNA was synthesized by reverse transcription according to the PrimeScript<sup>™</sup> RT reagent kit. Fluorescence quantification was performed using the TB Green<sup>™</sup> Premix Ex Taq<sup>™</sup> II kit and primers. PCR reactions were performed using a fully-automated medical PCR analysis system (SLAN-96P) to derive C<sub>t</sub> values and determine the relative expression of each gene using the  $2^{-\Delta\Delta C_t}$  method. The primer sequences are shown in Table 1.

## 2.10 Western blot analysis

A western blot analysis was used to examine the expression behavior of GLUT2, pancreatic/duodenal homeobox-1 (PDX1), and insulin (INS) proteins in different culture environments. The cells were collected and lysed in an ice bath for 10 min with radioimmunoprecipitation assay kit buffer. The samples were centrifuged at 4 °C and the supernatant was transferred into EP tubes. The proteins were then separated using 10% SDS polyacrylamide gel electrophoresis (SDS-page) and transferred to polyvinylidene difluoride (PVDF) membranes. After blocking with 5% bovine serum albumin (BSA) for 1 h, the primary antibody was incubated overnight at 4 °C. The horseradish peroxidase-labeled secondary antibody was added at room temperature and incubated for 2 h. The PVDF membrane was immersed in a luminescent solution and observed using an enhanced chemiluminescence detection system (Bio-Rad, Chemidoc XRS).

## 2.11 Signaling pathway analysis under different culture methods

We further examined the expression of the proteins in the phosphoinositide 3-kinase (PI3K)/serine/threonine protein kinase (AKT)/forkhead transcription factor FKHR (FoxO1)/pancreatic and duodenal homeobox 1 (PDX1) signaling pathway. After extracting the proteins, the expression of PI3K, AKT, phosphorylated AKT (p-AKT), FoxO1, phosphorylated FoxO1 (p-FoxO1), and PDX1 was detected by western blotting. The antibodies used were anti-PI3K, anti-AKT, anti-p-AKT, anti-FoxO1, anti-P-FoxO1, anti-PDX1, and anti-GAPDH. The grayscale

**Table 1** Primers used for qPCR

Gene	Forward primer	Reverse primer
GAPDH	CCAGTATGACTCCACTCACG	GACTCCACGACATACTCAGC
GLUT2	TCAGAAGACAAGATCACCGGA	GCTGGTGTGACTGTAAGTGGG
PDX1	CCCCAGTTTACAAGCTCGCT	CTCGGTTCCATTCGGGAAAGG
INS2	GCTTCTTCTACACCCCATGTC	AGCACTGATCTACAATGCCAC

values of the target proteins were analyzed using ImageJ software and normalized to GAPDH. The phosphorylation levels of AKT (p-AKT/AKT) and FoxO1 (p-FoxO1/FoxO1) were calculated.

### 2.12 Signaling pathway analysis under alginate hydrogel culture with different concentration

Various cell signaling pathways may be affected by the concentration of the hydrogel. The cells were encapsulated with different concentrations of hydrogel (0.5, 1.0, 2% w/v) to further study the effect of hydrogel-encapsulated MIN6 cells on PI3K/AKT/FoxO1 signaling pathway. The expressions of PI3K, AKT, P-AKT, FoxO1, P-FoxO1 and PDX1 was detected using western blotting. Image J was used to measure the optical density of each band for quantitative analysis.

### 2.13 Statistical analysis

All data were obtained from three independent experiments. The data were expressed as mean  $\pm$  standard deviation. Images were processed using GraphPad Prism 8.0 software (GraphPad Software, San Diego, CA, USA). Comparisons between groups were performed using a two-way analysis of variance with the Tukey test. Statistical significance was set at  $p < 0.05$ .

## 3 Results

### 3.1 MIN6 cells formed cell spheroids on the agarose microporous matrix

Islet size has been reported to be a critical contributor to the function of islet cells in secreting islet protein. The optimal size for clinical islet transplantation is 200  $\mu\text{m}$  [18]. Therefore, we explored the effect of four cell inoculation densities ( $7 \times 10^4$ ,  $1 \times 10^5$ ,  $3 \times 10^5$ ,  $6 \times 10^5$  cells/mL) on islet size. As shown in Fig. 1A, the MIN6 cells formed regular and tight islet-like spheroid in the microwell arrays at different inoculation densities, and the size of the aggregates were proportional to the initial cell density (Fig. 1B). After 5 days of culture, the aggregates were close to 200  $\mu\text{m}$  in size at a density of  $3 \times 10^5$  cells/

mL; therefore, we chose it as a model to continue exploring the effects of culture time on the size of the aggregates. The spheroid size increased from  $94 \pm 4.2$  to  $186 \pm 4.9$   $\mu\text{m}$  when the culture time was increased from 1 to 5 days; and the diameter of the spheroid increased to  $252 \pm 4.3$   $\mu\text{m}$  as the culture period was prolonged to 7 days (Fig. 1C, D). Therefore, we selected cell spheroids with a cell density of  $3 \times 10^5$  cells/mL and cultured them until Day 5 for functional validation in subsequent experiments.

### 3.2 Impact of hydrogel concentration on the viability and proliferation of MIN6 cells

We further examined the potential effect of the concentration of the hydrogel on the viability and proliferation of MIN6 cells (Fig. 2). We selected 0.5%, 1% and 2% concentrations of alginate gels as the models and observed the cell behavior after they has been encapsulated by the gels. There were no differences in the numbers of dead cells among the three concentration groups (Fig. 2A). However, larger live cell clumps were found in the 0.5% alginate group. Furthermore, the cells in the 2% alginate group presented as single cells, indicating that the high hydrogel concentration was not conducive for maintaining cellular proliferation. In addition, 0.5% and 1% alginate were found to be favorable for cell proliferation for 1 or 3 days of culture, and the 1% group was more favorable for long-term cell culture than the 0.5% group (5 and 7 days of culture) (Fig. 2B). The 0.5% alginate group had less structural rigidity after long-term culture, and it was difficult to maintain its overall structure at a later stage of culture. Therefore, we selected the 1% alginate gel group for this study.

### 3.3 Surface morphology of two 3D MIN6 models

As shown in Fig. 3A, B, the cells on the surface of the cell spheroids were closely connected and fused with each other. The spheroids remained regular in shape after collection, fixation, and dehydration, which further confirmed that the cells were closely clustered into a microtissue, such as an islet. As shown in Fig. 3C, D, the cross-sections of the alginate microbeads showed that the MIN6 cells grew in spherical clusters on the hydrogel surface. As shown in Fig. 3E, the dispersed cells encapsulated in 1% sodium

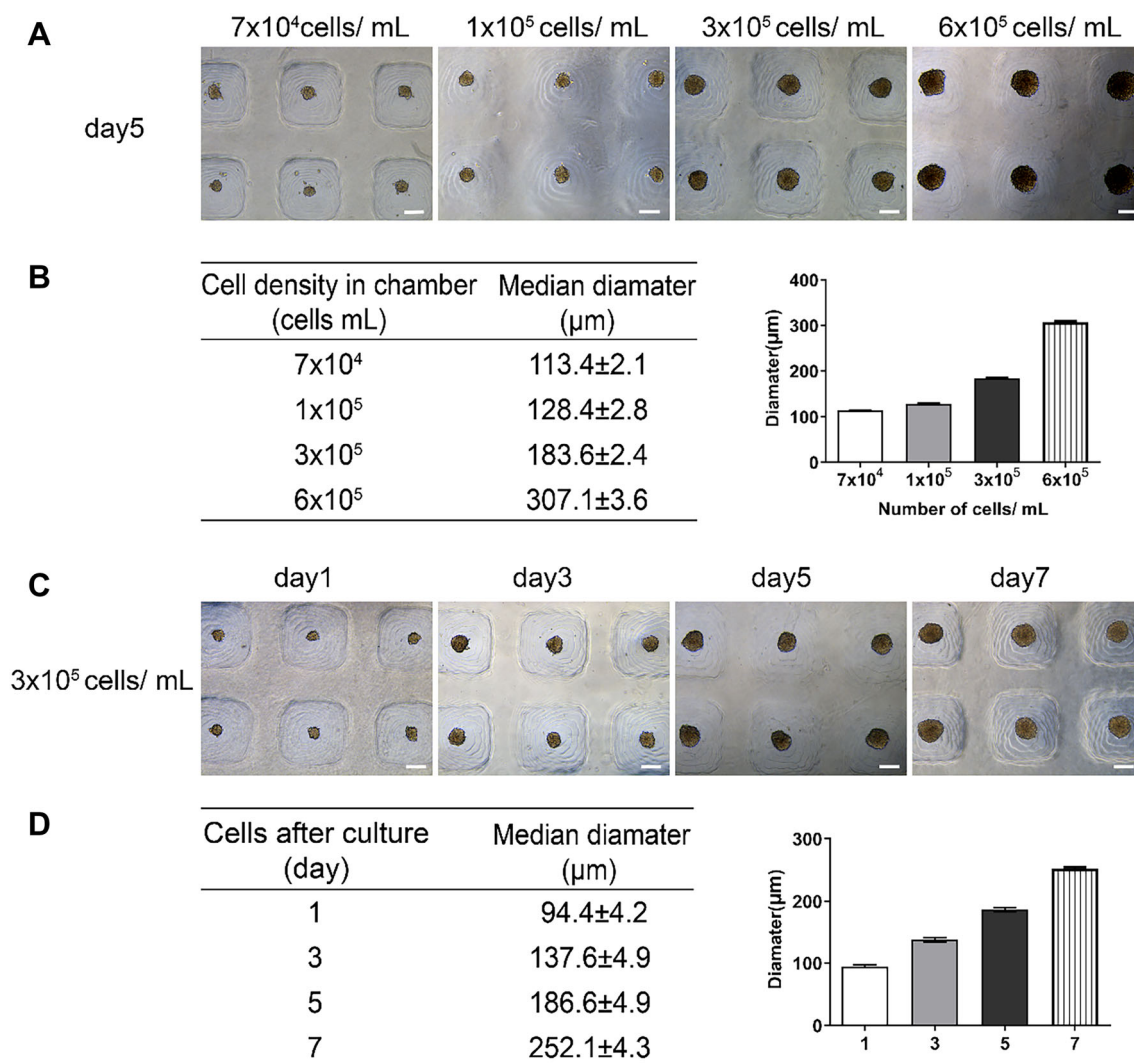


**Fig. 1** MIN6 cells spheroids formed in the agarose microwell array. **A** Optical image of MIN6 spheroids cultured in microwell arrays for 5 days (scale bar, 250 μm); **B** Size distribution of the spheroid affected by the initial cell density; **C** Optical image of the spheroid

with the initial cell density of  $3 \times 10^5$  cells/mL (scale bar, 250 μm); **D** Diameter of the spheroids affected by the culture period. 2D group (blank bars), Spheroid group (gray bars), and hydrogel group (black bars). The scale bar in (A) and (C) is 250 μm

alginate proliferated to form clusters. The alginate cell bulk were showed in Fig. 3F.

### 3.4 Effects of 3D culture on the viability and proliferation of MIN6

The cells were stained with AM/PI working solution and imaged with laser confocal laminar scan. The 2D culture conditions facilitates the viability and growth of MIN6 within 5 days (Fig. 4A). Furthermore, when the cells were cultured in spheroid form, they maintained high viability within the first 5 days, and no dead cells were observed; however, when the culture time was extended to 7 days, abundant dead cells were found inside the spheroid (Fig. 4B). The alginate hydrogel-encapsulated cell maintained a high survival rate in the first 5 days of culture.

However, dead cells appeared on Day 7, and the survival rate decreased (Fig. 4C). The CellTiter-Glo<sup>®</sup> 3D kit was used to evaluate the proliferation behavior of cells in different culture environments. The spheroid and alginate hydrogel-encapsulated cells in the 3D culture exhibited faster proliferation than those in the 2D culture (Fig. 4D).

### 3.5 Glucose stimulates insulin secretion

We investigated the effects of glucose concentration on the secretion of islets in the MIN6 cells. The stimulatory glucose (25.5 mM) environment was more favorable for β cell insulin secretion than the low glucose (5.5 mM) environment under the three culture conditions (Fig. 5), indicating that the MIN6 cells were more sensitive to high-sugar stimulation. In addition, the insulin secretion level of the

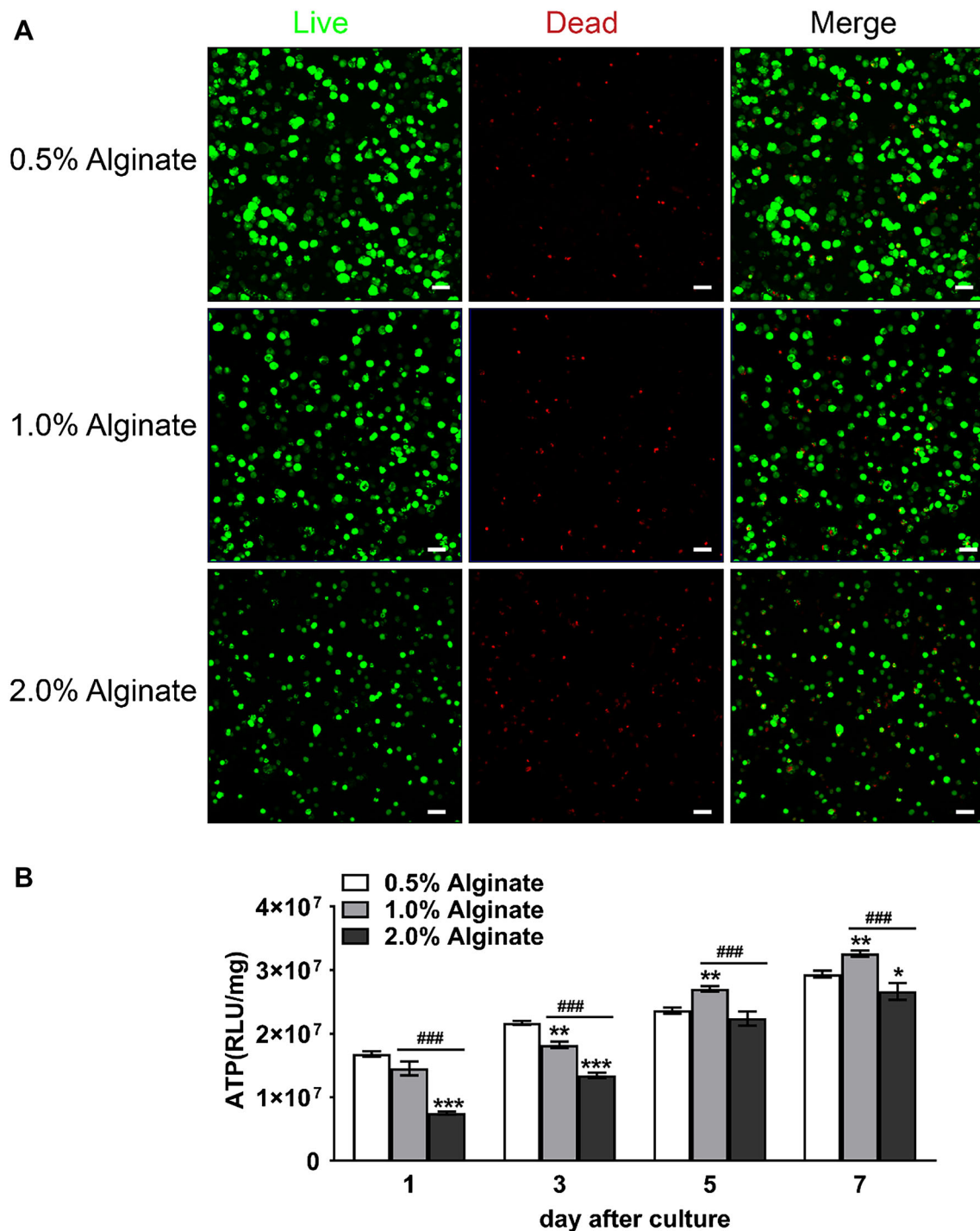


**Fig. 2** Impact of hydrogel concentration on the viability and proliferation of MIN6 cells. **A** Live/dead staining of MIN6 cells encapsulated in different concentration of alginate hydrogel on 2D cell culture plates for 5 days. Scale bar, 50  $\mu$ m; **B** Growth behavior of

MIN6 cells in the alginate hydrogel. 2D group (blank bars), Spheroid group (gray bars), and hydrogel group (black bars). Values are mean  $\pm$  standard error of the mean,  $n = 3$ . \* $p < 0.05$ , \*\* $p < 0.01$ , \*\*\* $p < 0.001$  vs. 0.5% alginate. ### $p < 0.001$  vs. 2% alginate

alginate hydrogel-encapsulated cells in the low-sugar environment were significantly higher than those the 2D culture ( $p < 0.05$ ) and spheroid groups ( $p < 0.01$ ). The insulin secretion levels of the cells in the spheroid group were also higher than those in the 2D culture group, with

no statistical difference. This trend is consistent under the high-glucose conditions. The glucose stimulation indexes (GSI; ratio between insulin secretion at 25.5 mM and at 5.5 mM glucose) were slightly higher in the case of hydrogel conditions (Table 2); However, there was no

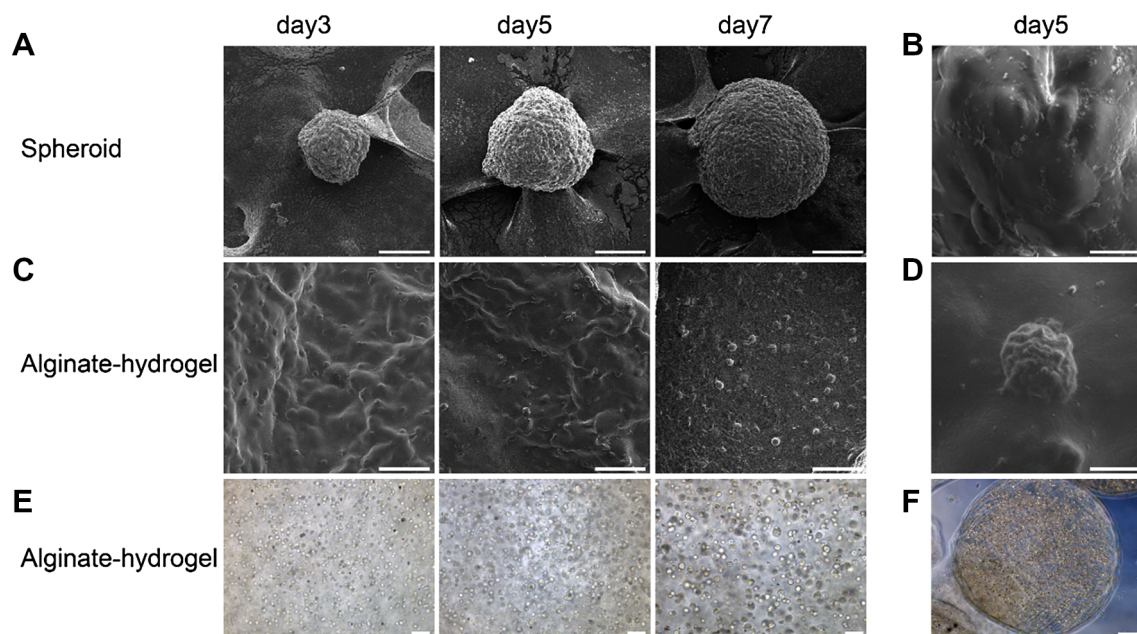


**Fig. 3** Surface morphology of the two cell models. **A** The surface structure of the MIN6 cell spheroids were observed by SEM on Days 3, 5 and 7. **B** Local magnification scan of cell spheroids group on day 5. **C** SEM images of the cross-section of the alginate gel beads on Days 3, 5 and 7. **D** Local magnification scan of the alginate-cell group

on Day 5. **E**, **F** MIN6 cells were encapsulated in 1% alginate, and imaged in a bright field under an inverted microscope on Days 1, 3, 5 and 7. Scale bars: 100  $\mu$ m (**A**, **C**). Scale bars: 10  $\mu$ m (**B**, **D**). Scale bars: 100  $\mu$ m (**E**). Scale bars: 250  $\mu$ m (**F**)

significant difference in the amount of GSI secreted by the cells in 3D spheroid and alginate gel culture conditions.

### 3.6 Gene and protein expression of $\beta$ cell transcription factors

We further investigated whether the culture system regulated the expression of  $\beta$  cell related genes, including GLUT2, PDX1, INS2. The spheroid and hydrogel groups could significantly upregulate the expression of islet secretion-related genes in the MIN6 cells, and their expression levels were higher than those in the 2D group (Fig. 6A). The expression level of GLUT2 in the cell spheroid and hydrogel groups was higher than that in the 2D group; however, the difference was not statistically significant. In addition, the expression levels of PDX1 and INS2 were the highest in the hydrogel-encapsulated cells ( $p < 0.001$ ), and those in the spheroid group were also significantly higher than those in the 2D group ( $p < 0.05$ ). As shown in Fig. 6B, the western blot experiments confirmed the high expression of PDX1 and INS in the 3D culture, and the highest expression levels were found in the hydrogel group, which was consistent with the PCR results.

### 3.7 PI3K/AKT/FoxO1 signaling pathway in different models of MIN6 cells

The expression levels of PI3K, p-AKT/AKT proteins were significantly higher in the hydrogel group than in the other two groups (Fig. 7). Their expression levels were also higher in the spheroid group than in the 2D group, although there was no significant difference between them. Meanwhile, we examined the expression levels of FoxO1 and P-FoxO1 proteins. According to the results, the hydrogel-encapsulated cells exhibited the highest P-FoxO1/FoxO1 and PDX1 protein expression levels (Fig. 7). Therefore, we hypothesize that 3D cultures promoted the insulin secretory function of MIN6 cells by activating PI3K, catalyzing the phosphorylation of AKT and FoxO1, and upregulating the expression of PDX1.

### 3.8 Effects of alginate concentration on signaling of PI3K/AKT/FoxO1 pathway

To further confirm the role PI3K/AKT/FoxO1 pathway in the 3D MIN6 cell culture, the effects of variable concentration of alginate on PI3K/AKT/FoxO1 signaling pathway were investigated. Western blot was used to detect the expression of key proteins, including PI3K, AKT, p-AKT, FoxO1, p-FoxO1 and PDX-1 (Fig. 8). The results showed that the PI3K expression was not significant different between the 0.5% and 1% alginate concentrations, but was



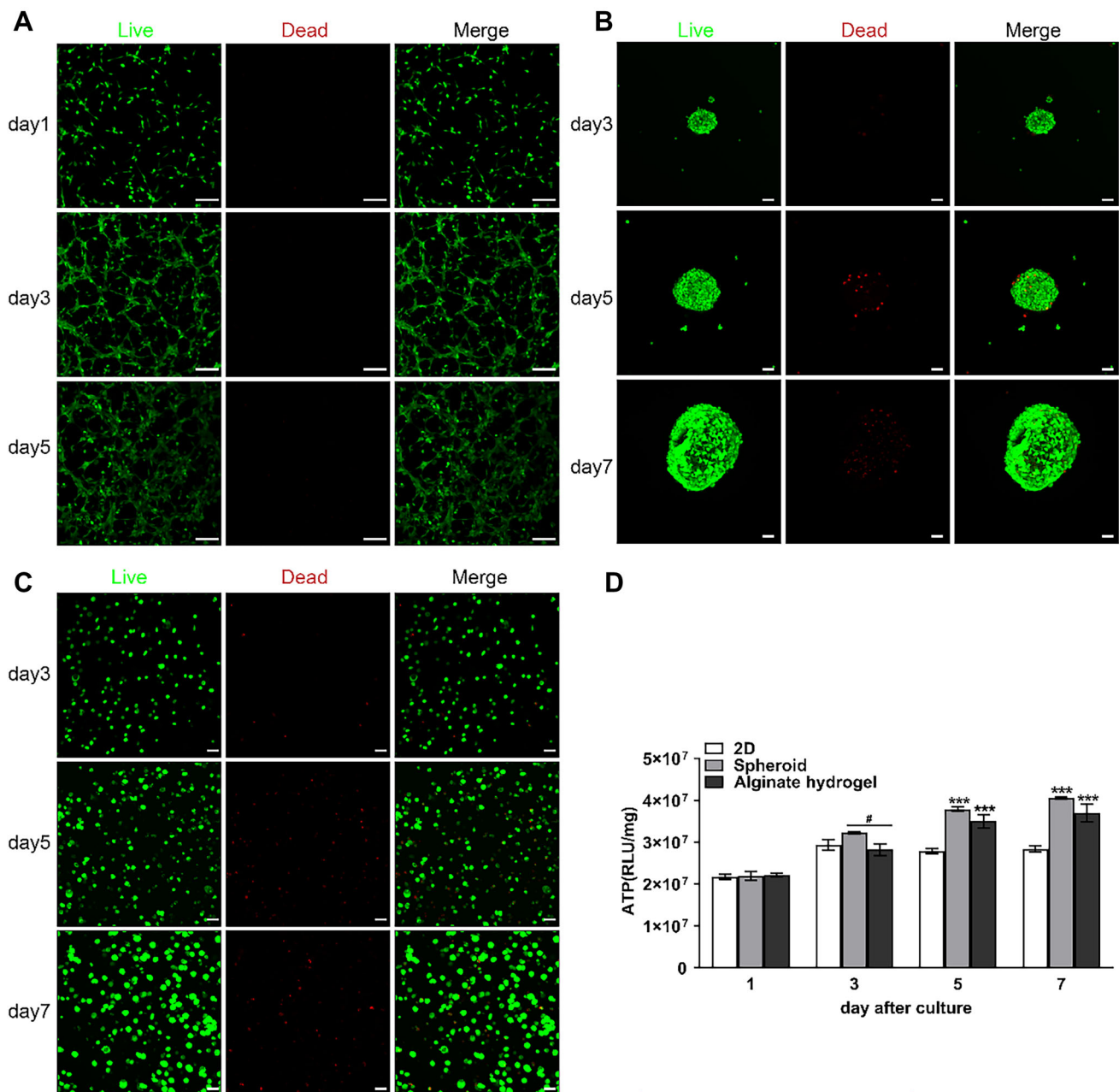


**Fig. 4** Effects of 3D culture on the viability and proliferation of MIN6. The viability of **A** the MIN6 cells cultured on 2D cell culture plate (scale bar, 100  $\mu$ m), **B** microwell arrays (scale bar, 50  $\mu$ m), and **C** an alginate hydrogel matrix (scale bar, 50  $\mu$ m). **D** Proliferation rate

of MIN6 in different culture environments. 2D group (blank bars), Spheroid group (gray bars), and hydrogel group (black bars). Values are the mean  $\pm$  standard error of the mean,  $n = 3$ . \*\*\* $p < 0.001$  vs. 2D. # $p < 0.05$  vs. Spheroid

significantly reduced by the 2% alginate concentration ( $p < 0.05$ ). The expression of p-AKT/AKT, p-FoxO1/FoxO1, PDX1 was the highest with the 1% alginate concentration ( $p < 0.05$ ), and there was no significant difference between the expression level of the 0.5% and 2% alginate concentration. The 1% hydrogel, therefore, enhanced the viability of MIN6 cells and PI3K/AKT/FoxO1 signaling pathway.

#### 4 Discussion

Compared to the MIN6 cultured in a 2D system, those in the spheroids or encapsulated in the alginate hydrogel exhibit higher cell viability and enhanced insulin secretion and GSIS response. Although the values of GSI were not significantly different, the GSIS response may be explained by different baseline secretion due to the changes in the surrounding microenvironment. The gene and protein

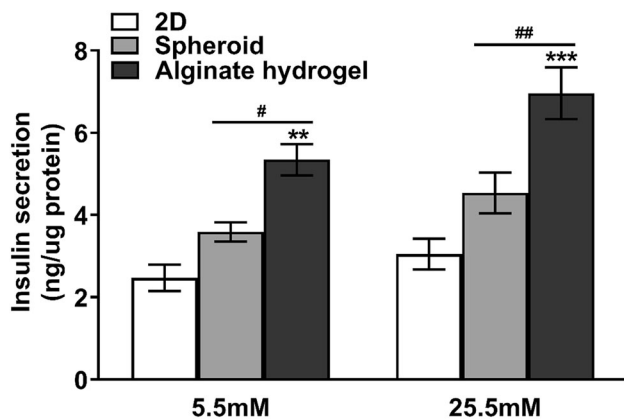


**Fig. 5** Glucose stimulates insulin secretion. Insulin secretion of MIN6 cells stimulated by glucose for 5 days. 2D group (blank bars), spheroid group (gray bars), and hydrogel group (black bars). Values are mean  $\pm$  standard error of the mean,  $n = 3$ . \*\* $p < 0.01$ , \*\*\* $p < 0.001$  vs. 2D. # $p < 0.05$ , ## $p < 0.01$  vs. Spheroid

**Table 2** Glucose stimulated index (insulin secreted by cells at high glucose stimulation condition vs insulin at low glucose stimulation) standardized to the amount of protein from cells measured by GSIS and ELISA assay

1%	Condition alginate	2D	Spheroids
GSI	1.24 $\pm$ 0.05	1.32 $\pm$ 0.08	1.32 $\pm$ 0.07

Values are mean  $\pm$  SD,  $n = 5$

expression of functional markers such as PDX1 and INS2 in MIN6 cells were also upregulated in the two 3D models compared with those in the 2D culture. That is consistent with the results published by Chowdhury [39], who reported that Min6 cell spheroids were more responsive to GSIS than cells in 2D culture. The PI3K inhibitor reduced GSIS reaction of Min6 cell spheroids, markedly but had no obvious effect on the 2D cell culture.

The effects of variable alginate concentration on the MIN6 cells activity were also investigated. The results showed that 1% alginate hydrogel was more suitable for long-term Min6 cell culture, this was consistent with Sneha et al. [40, 41]. The authors showed that low-concentration alginate hydrogels (0.5% and 1% alginate) were suitable for long-term 3D culture of mouse embryonic cells. The lowest cell proliferation and viability rates were observed in the 1.5% alginate group. Low-concentration alginate hydrogels tend to degrade rapidly. The authors concluded that 1% alginate hydrogel was the most suitable choice for 3D encapsulation of mouse embryonic cells [34].

We found that Min6 cells in the spheroids and 1% alginate proliferated more than those in the 2D culture, whereas there were no statistical differences between the

two 3D groups. However, the 1% alginate hydrogel-encapsulated cells showed significantly higher basal insulin secretion levels and GSIS than the spheroids. In addition, the expression of  $\beta$  cell related genes (GLUT2, PDX1, INS2) varied in the different models. The GLUT2 expression generally remained unchanged among the models. INS2 expression was upregulated in the 3D culture compared to that in the 2D culture, but there were no marked differences in the two 3D models. PDX1 expression was increased in 3D culture and the alginate-encapsulated MIN6 cells showed a higher PDX1 expression than the MIN6 spheroids. GLUT2 is a carrier protein for glucose transport, and its expression is related to transport velocity [42]. PDX1 plays an important role in  $\beta$  cell transcription and insulin secretion [43, 44]. INS2 is partially proportional to insulin level [45, 46]. The protein expression levels of PI3K, p-AKT/AKT, and p-FoxO1/FoxO1 in the 1% alginate-encapsulated cells were significantly higher than those in spheroids and 2D culture. To confirm the role of PI3K/AKT/FoxO1 signaling on MIN6 functions in different models, we investigated the effects of variable alginate concentration on the PI3K/AKT/FoxO1 signaling in the encapsulated cells. The 1% alginate-encapsulated MIN6 cells showed a higher expression of PI3K/AKT/FoxO1 signal molecules than those in 0.5% or 2% alginate.

The PI3K/AKT/FoxO1 signaling pathway mediated insulin secretion by promoting PDX1 expression [47–49]. PI3K/AKT regulates the proliferation and metabolism of pancreatic  $\beta$  cells [50, 51]. AKT acts as the main downstream effector of PI3K [52, 53]. In addition, FoxO1 is highly expressed in human and mouse pancreatic  $\beta$  cells and is regulated by phosphorylated AKT [54–56]. Phosphorylation of FoxO1 leads to up-regulate the expression of PDX1 and promoting insulin transcription [57, 58]. Our results suggest that 1% alginate hydrogel encapsulating  $\beta$  cells exhibit a higher insulin response than cell spheroid, and the underlying mechanisms may be related to enhanced PDX1 expression through PI3K/AKT/FoxO1 pathway. Hence, as represented by the MIN6 cells, the alginate encapsulation system may have better potential for  $\beta$  cells transplantation than in spheroids.

Similarly, Pei et al. [59] reported that islet-like cell aggregates generated by a rotating culture system exhibited enhanced GSIS level compared with the 2D culture system, the underlying mechanism involved the upregulation of connexin 36 expression (CX36), inhibition of the RhoA/ROCK pathway, promotion of F-actin remodeling, and increase in insulin secretion. MIN6 in the 3D culture system may also relate to the MLCK-ROCK/ $\beta$ -catenin pathway. In contrast, Bernard [60] found that the cell viability and GSIS ability of MIN6 spheroid encapsulated in a polyethylene glycol acrylate hydrogel (PEGDA) were

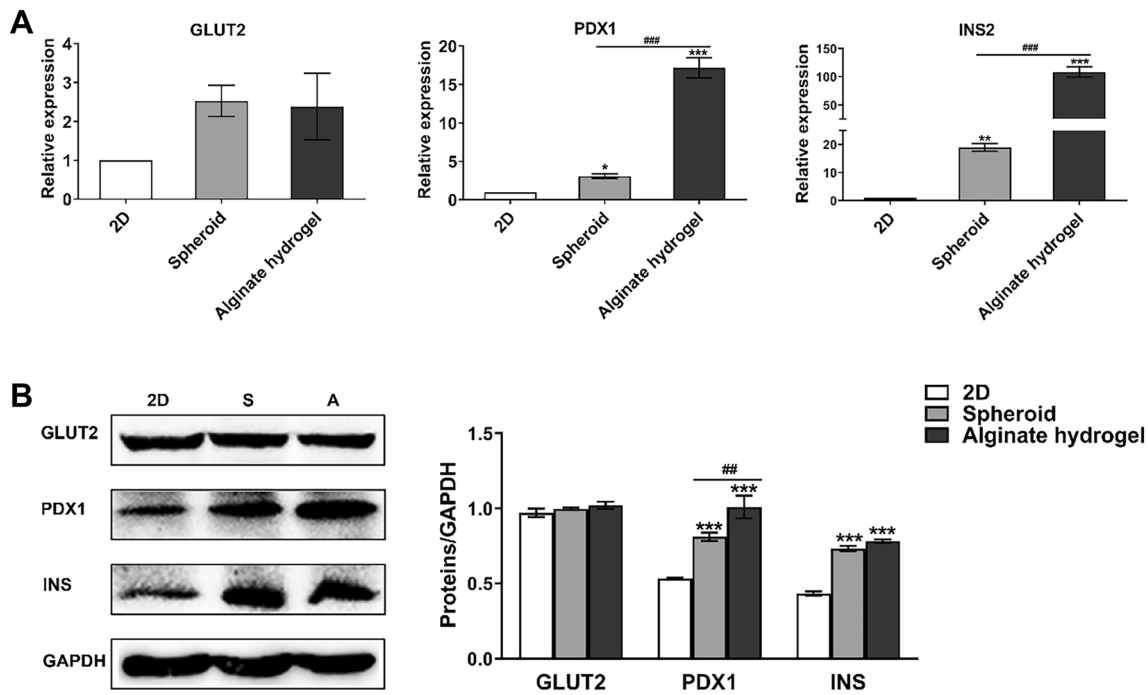


**Fig. 6** A, B Gene and protein expression of  $\beta$  cell transcription factors. Gene and protein expression of MIN6 cells in 2D culture, microwell array and alginate hydrogel matrix. 2D group (blank bars), Spheroid group (gray bars), and hydrogel group (black bars). The

relative gene and protein expression were calculated after normalization to the GAPDH. Values are mean  $\pm$  standard error of the mean,  $n = 3$ . \* $p < 0.05$ , \*\* $p < 0.01$ , \*\*\* $p < 0.001$  vs. 2D. ### $p < 0.05$ , #### $p < 0.01$  vs. Spheroid

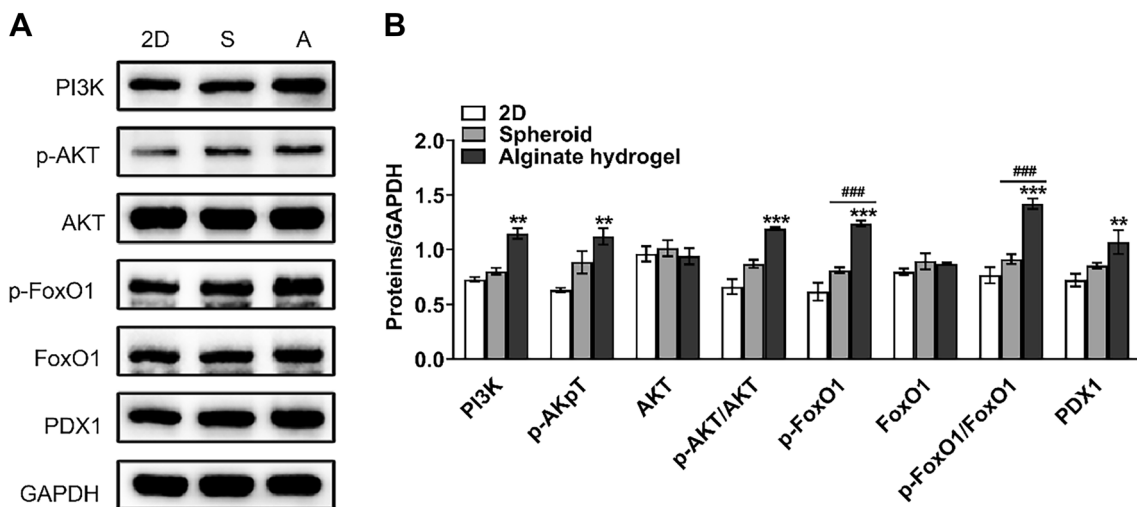


**Fig. 7** The potential effect of culture environment on the expression of protein in the PI3K/AKT/FoxO1 signaling pathway. The expression of PI3K, AKT and p-AKT, FoxO1, p-FoxO1, PDX1 in the MIN6 cells were quantitatively detected by a western blot. 2D group (blank

bars), Spheroid group (gray bars), and hydrogel group (black bars). The relative protein expression was calculated after normalization to the GAPDH. Values are mean  $\pm$  Standard error of the mean,  $n = 3$ . \*\* $p < 0.01$ , \*\*\* $p < 0.001$  vs. 2D. ### $p < 0.001$  vs. Spheroid

significantly higher than those of dispersed MIN6 cells encapsulated in PEGDA. The UV-crosslinked synthetic PEGDA may have impaired cell viability, as the encapsulated dispersed cells were only 20% viable after 7 days in culture. In addition, there was no cell proliferation or increase in the diameter of the spheroid in PEGDA

hydrogel. Therefore, we speculate that the difference of between the study by Bernard and ours may be due to the different properties of the two hydrogels.

Compared with the cell spheroid, the alginate-encapsulated cells would be stimulated by mechanical stress caused by the hydrogel during the growth and proliferation.

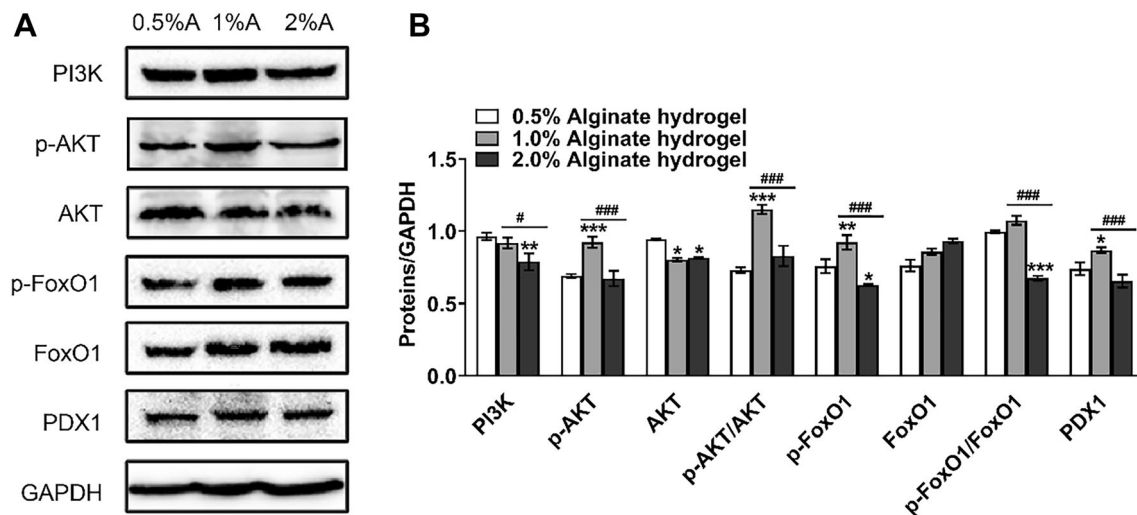


**Fig. 8** **A, B** Effect of alginate gel concentration on the signaling pathway of MIN6 cells. The expression of PI3K, AKT and p-AKT, FoxO1, p-FoxO1, PDX1 in MIN6 cells were quantitatively detected by western blot. 2D group (blank bars), Spheroid group (gray bars),

and hydrogel group (black bars). The relative gene and protein expression were calculated after normalization to the GAPDH. Values are mean  $\pm$  Standard error of the mean,  $n = 3$ . \* $p < 0.05$ , \*\* $p < 0.01$ , \*\*\* $p < 0.001$  vs. 2D. # $p < 0.05$ , ### $p < 0.001$  vs. Spheroid

Nyitray et al. [59] observed the effect of microenvironmental mechanical stress on Min6 with different concentrations of polyacrylamide, and found that the insulin expression of cells in 0.1 kPa scaffolds was significantly higher than that in 10 kPa scaffolds. The corresponding mechanism involved the MLCK and ROCK mechanotransduction pathways, which may have eventually influenced  $\beta$ -catenin signaling and regulated insulin secretion. The  $\beta$ -catenin activator could block the overexpression of insulin in the 0.1 kPa scaffold, and the inhibition of insulin expression in the 10 kPa scaffold was reversed by  $\beta$ -catenin inhibitors [61]. Our study demonstrated that the expression of the protein in the PI3K/AKT/FoxO1 pathway and PDX1 was higher in the 1% alginate-encapsulated MIN6 than that in the 0.5% and 2% sodium alginate-encapsulated cells. Adele et al. reported that the Young's Modulus of 0.5%, 1% and 2% alginate was  $1.85 \pm 0.08$  kPa,  $2.85 \pm 0.25$  kPa,  $5.29 \pm 0.25$  kPa, respectively [62]. And the Young's Modulus of spheroids has been reported to be  $84 \pm 78$  Pa [63]. These studies together with our results, demonstrate that a better understanding of the mechanisms underlying the functions of  $\beta$  cells is necessary to elucidate their optimal functions involving signaling pathways, including PI3K/AKT/FOXO1. Cell-cell interactions of pancreatic  $\beta$  cells are important for maintaining islet function [40], however, our study showed that MIN6 cells dispersed in 1% alginate continue to proliferate and aggregate, just as spheroids, and exert cell-cell interactions. It is reasonable that these two factors may contribute to the improved functions of the alginate encapsulation of MIN6 cells over spheroids,

including cell-cell interactions and mechanical stimulation from the matrix.

There are several limitations in this study. The MIN6 cell line was established using murine insulinomas. The endocrine function of MIN6 cells is similar to that of pancreatic tissue, which makes them ideal models for studying the function of islet cells. However, they may rarely be used in future clinical islet transplantations. Islets can be easily dissociated into single cells and reaggregated into PIs with controlled sizes and cell compositions. PIs have been demonstrated to improve viability and function both *in vitro* and *in vivo*, similar to native islets [64]. For example, human islets have been dissociated and reaggregated into uniform, size-controlled islets via centrifugal-forced aggregation (CFA-PIs) with greatly enhanced *in vitro* function. Furthermore, the performance of CFA-PIs has been compared favorably with that of native human islets after transplantation in mouse kidney capsules [29]. In our study, although MIN6 cells were used to demonstrate the differences between two common 3D models of artificial pancreatic islets, the adoption of single cells from human islets would not provide more valuable information for clinical applications.

Besides, to confirm the functions of pancreatic cells in different 3D models, those pancreatic grafts should be transplanted in diabetic animals to examine the GSIS, glucose tolerance testing (GTT), etc. For transplantation of alginate-encapsulating cells including MIN6 in diabetic animals, an improved insulin secretion has been demonstrated [65–67]. However, there were no reports about direct transplanting MIN6 spheroids in diabetic animals as we can find. Since MIN6 cells were established from

insulinoma, it is imaginable that MIN6 cells would proliferate rapidly and develop tumors after transplantation, which would not happen in alginate-encapsulating cells because of the confinement of alginate. By far, the insulin secretory functions of MIN6 were usually investigated *in vitro* except alginate-encapsulating cells [45, 68]. Alternatively, islets were considered preferable for direct transplantation in clinical application [7] or animal experiments [29]. Since that, islets collected from pancreas should be considered for transplantation to confirm the conclusions of the present study, which may deserve further research and provide substantial evidence for clinical translation.

In summary, this study compared the behavior of cells from the pancreatic  $\beta$  cell line MIN6 in spheroids with that of cells encapsulated in alginate, which comprise two common *in vitro* models for artificial pancreatic islets. Cell proliferation and the expression of islet-related genes were significantly enhanced in the two 3D-culture compared to those in the 2D cultures. Compared with the spheroids, the MIN6 cells encapsulated in 1% alginate exhibited a higher GSIS, expression of  $\beta$ -cell-related markers, and more proliferation. In addition, the 3D culture could promote insulin secretion by upregulating PDX1 expression through the activation of the PI3K/AKT/FoxO1 signaling pathway. Cells encapsulated in 1% alginate further showed higher PDX1 expression and PI3K/AKT/FoxO1 signaling than those in the spheroids and those encapsulated in 0.5% and 2% alginate. Therefore, this study provides insights into selecting preferable 3D culture systems for  $\beta$  cells for artificial pancreatic islet transplantation.

**Acknowledgments** The work was supported by National Natural Science Foundation of China (Grant No.81860327, 81860642), Academic and technical Leaders Program in Jiangxi Province (Grant No.20204BCJL22052). Key Laboratory Program in Jiangxi Province (Grant No.20202BCD42012).

**Author contributions** Study conception and design: XX Chao, FRZ, JWH; Acquisition of data: YRY, RJX, JNZ, MH; Analysis and interpretation of data, critical revision: HY, DL, WJP.

#### Declarations

**Conflicts of interest** The authors declare no conflict of interest.

**Ethical statement** There are no animal experiments carried out for this article.

#### References

- Li W, Huang E, Gao S. Type 1 diabetes mellitus and cognitive impairments: a systematic review. *J Alzheimers Dis.* 2017;57:29–36.
- Zhang W, Wu SZ, Zhou J, Chen HM, Gong YL, Peng FF, et al. Parathyroid hormone-related peptide (1–34) reduces alveolar bone loss in type 1 diabetic rats. *Arch Oral Biol.* 2017;83:13–9.
- Luo X, Wu J, Jing S, Yan LJ. Hyperglycemic stress and carbon stress in diabetic glucotoxicity. *Aging Dis.* 2016;7:90–110.
- Mayer-Davis EJ, Lawrence JM, Dabelea D, Divers J, Isom S, Dolan L, et al. Incidence trends of type 1 and type 2 diabetes among youths, 2002–2012. *N Engl J Med.* 2017;376:1419–29.
- De Paoli T, Rogers PJ. Disordered eating and insulin restriction in type 1 diabetes: a systematic review and testable model. *Eat Disord.* 2018;26:343–60.
- Beck RW, Riddlesworth TD, Ruedy KJ, Kollman C, Ahmann AJ, Bergenstal RM, et al. Effect of initiating use of an insulin pump in adults with type 1 diabetes using multiple daily insulin injections and continuous glucose monitoring (DIAMOND): a multicentre, randomised controlled trial. *Lancet Diabetes Endocrinol.* 2017;5:700–8.
- Shapiro AMJ, Pokrywczynska M, Ricordi C. Clinical pancreatic islet transplantation. *Nat Rev Endocrinol.* 2017;13:268–77.
- Cui SS, Duan LJ, Li JF, Qin YZ, Bao SQ, Jiang X. The factors influencing the renal glucose threshold in patients with newly diagnosed type 2 diabetes mellitus. *Diabetes Metab Syndr.* 2021;14:4497–503.
- Hering BJ, Clarke WR, Bridges ND, Eggerman TL, Alejandro R, Bellin MD, et al. Phase 3 trial of transplantation of human islets in type 1 diabetes complicated by severe hypoglycemia. *Diabetes Care.* 2016;39:1230–40.
- Orive G, Emerich D, Khademhosseini A, Matsumoto S, Hernández RM, Pedraz JL, et al. Engineering a clinically transplantable bioartificial pancreas to treat type I diabetes. *Trends Biotechnol.* 2018;36:445–56.
- Vériter S, Gianello P, Dufrane D. Bioengineered sites for islet cell transplantation. *Curr Diab Rep.* 2013;13:745–55.
- Speight J, Reaney MD, Woodcock AJ, Smith RM, Shaw JA. Patient-reported outcomes following islet cell or pancreas transplantation (alone or after kidney) in type 1 diabetes: a systematic review. *Diabetic Med.* 2010;27:812–22.
- Gamble A, Pepper AR, Bruni A, Shapiro AMJ. The journey of islet cell transplantation and future development. *Islets.* 2018;10:80–94.
- Cunha J, Gysemans C, Gillard P, Mathieu C. Stem-cell-based therapies for improving islet transplantation outcomes in type 1 diabetes. *Curr Diabetes Rev.* 2018;14:3–13.
- Menger MM, Nalbach L, Wrublewsky S, Glanemann M, Gu Y, Laschke MW, et al. Darbepoetin- $\alpha$  increases the blood volume flow in transplanted pancreatic islets in mice. *Acta Diabetol.* 2020;57:1009–18.
- Anazawa T, Okajima H, Masui T, Uemoto S. Current state and future evolution of pancreatic islet transplantation. *Ann Gastroenterol Surg.* 2019;3:34–42.
- Richardson T, Kumta PN, Banerjee I. Alginate encapsulation of human embryonic stem cells to enhance directed differentiation to pancreatic islet-like cells. *Tissue Eng Part A.* 2014;20:3198–211.
- Lehmann R, Zuellig RA, Kugelmeier P, Baenninger PB, Moritz W, Perren A, et al. Superiority of small islets in human islet transplantation. *Diabetes.* 2007;56:594–603.
- Giuliani M, Moritz W, Bodmer E, Dindo D, Kugelmeier P, Lehmann R, et al. Central necrosis in isolated hypoxic human pancreatic islets: evidence for postisolation ischemia. *Cell Transplant.* 2005;14:67–76.
- de Vos P, Faas MM, Strand B, Calafiore R. Alginate-based microcapsules for immunoisolation of pancreatic islets. *Biomaterials.* 2006;27:5603–17.
- Hauge-Evans AC, Squires PE, Belin VD, Roderigo-Milne H, Ramracheya RD, Persaud SJ, et al. Role of adenine nucleotides in

- insulin secretion from MIN6 pseudoislets. *Mol Cell Endocrinol*. 2002;191:167–76.
22. Rezania A, Bruin JE, Arora P, Rubin A, Batushansky I, Asadi A, et al. Reversal of diabetes with insulin-producing cells derived in vitro from human pluripotent stem cells. *Nat Biotechnol*. 2014;32:1121–33.
  23. Tan J, Liu L, Li B, Xie Q, Sun J, Pu H, et al. Pancreatic stem cells differentiate into insulin-secreting cells on fibroblast-modified PLGA membranes. *Mater Sci Eng C Mater Biol Appl*. 2019;97:593–601.
  24. Loomans CJM, Williams Giuliani N, Balak J, Ringnalda F, van Gorp L, Huch M, et al. Expansion of adult human pancreatic tissue yields organoids harboring progenitor cells with endocrine differentiation potential. *Stem Cell Reports*. 2018;10:712–24.
  25. Zhang D, Jiang W, Liu M, Sui X, Yin X, Chen S, et al. Highly efficient differentiation of human ES cells and iPS cells into mature pancreatic insulin-producing cells. *Cell Res*. 2009;19:429–38.
  26. Furuyama K, Chera S, van Gorp L, Oropeza D, Ghila L, Damond N, et al. Diabetes relief in mice by glucose-sensing insulin-secreting human  $\alpha$ -cells. *Nature*. 2019;567:43–8.
  27. Meivar-Levy I, Ferber S. Reprogramming of liver cells into insulin-producing cells. *Best Pract Res Clin Endocrinol Metab*. 2015;29:873–82.
  28. Rogers GJ, Hodgkin MN, Squires PE. E-cadherin and cell adhesion: a role in architecture and function in the pancreatic islet. *Cell Physiol Biochem*. 2007;20:987–94.
  29. Yu Y, Gamble A, Pawlick R, Pepper AR, Salama B, Toms D, et al. Bioengineered human pseudoislets form efficiently from donated tissue, compare favourably with native islets in vitro and restore normoglycaemia in mice. *Diabetologia*. 2018;61:2016–29.
  30. Tanaka H, Tanaka S, Sekine K, Kita S, Okamura A, Takebe T, et al. The generation of pancreatic  $\beta$ -cell spheroids in a simulated microgravity culture system. *Biomaterials*. 2013;34:5785–91.
  31. Maltman DJ, Przyborski SA. Developments in three-dimensional cell culture technology aimed at improving the accuracy of in vitro analyses. *Biochem Soc Trans*. 2010;38:1072–5.
  32. Knight E, Przyborski S. Advances in 3D cell culture technologies enabling tissue-like structures to be created in vitro. *J Anat*. 2015;227:746–56.
  33. Boland BB, Rhodes CJ, Grimsby JS. The dynamic plasticity of insulin production in  $\beta$ -cells. *Mol Metab*. 2017;6:958–73.
  34. Ravi M, Paramesh V, Kaviya SR, Anuradha E, Solomon FD. 3D cell culture systems: advantages and applications. *J Cell Physiol*. 2015;230:16–26.
  35. Duval K, Grover H, Han LH, Mou Y, Pegoraro AF, Fredberg J, et al. Modeling physiological events in 2D vs. 3D cell culture. *Physiology*. 2017;32:266–77.
  36. Zhang K, Manninen A. 3D cell culture models of epithelial tissues. *Method Mol Biol*. 2019;1926:77–84.
  37. Peng W, Unutmaz D, Ozbolat IT. Bioprinting towards physiologically relevant tissue models for pharmaceuticals. *Trends Biotechnol*. 2016;34:722–32.
  38. Namgung B, Ravi K, Vikraman PP, Sengupta S, Jang HL. Engineered cell-laden alginate microparticles for 3D culture. *Biochem Soc Trans*. 2021;49:761–73.
  39. Chowdhury A, Dyachok O, Tengholm A, Sandler S, Bergsten P. Functional differences between aggregated and dispersed insulin-producing cells. *Diabetologia*. 2013;56:1557–68.
  40. Oberai S, Teo A, Lim M, Ramamoorthi K, Hara J, Asuri PJAJ. Three-dimensional hydrogel encapsulated embryonic stem and carcinoma cells as culture platforms for cytotoxicity studies. *AIChE J*. 2015;61:3180–4.
  41. Sugiura S, Cha JM, Yanagawa F, Zorlutuna P, Bae H, Khademhosseini A. Dynamic three-dimensional micropatterned cell co-cultures within photocurable and chemically degradable hydrogels. *J Tissue Eng Regen Med*. 2016;10:690–9.
  42. Saleh LS, Carles-Carner M, Bryant SJ. The in vitro effects of macrophages on the osteogenic capabilities of MC3T3-E1 cells encapsulated in a biomimetic poly(ethylene glycol) hydrogel. *Acta Biomater*. 2018;71:37–48.
  43. Safi SZ, Qvist R, Ong G, Karimian H, Imran M, Shah I. Stimulation of  $\beta$ -adrenergic receptors plays a protective role via increased expression of RAF-1 and PDX-1 in hyperglycemic rat pancreatic islet (RIN-m5F) cells. *Arch Med Sci*. 2017;13:470–80.
  44. Spaeth JM, Walker EM, Stein R. Impact of Pdx1-associated chromatin modifiers on islet  $\beta$ -cells. *Diabetes Obes Metab*. 2016;18:123–7.
  45. Bynigeri RR, Mitnala S, Talukdar R, Singh SS, Duvvuru NR. Pancreatic stellate cell-potentiated insulin secretion from Min6 cells is independent of interleukin 6-mediated pathway. *J Cell Biochem*. 2020;121:840–55.
  46. Li Z, Yu P, Wu J, Tao F, Zhou J. Transcriptional regulation of early growth response gene-1 (EGR1) is associated with progression of nonalcoholic fatty liver disease (NAFLD) in patients with insulin resistance. *Med Sci Monit*. 2019;25:2293–3004.
  47. Huang X, Liu G, Guo J, Su Z. The PI3K/AKT pathway in obesity and type 2 diabetes. *Int J Biol Sci*. 2018;14:1483–96.
  48. Li B, Yang J, Lu Z, Liu B, Liu F. A study on the mechanism of rapamycin mediating the sensitivity of pancreatic cancer cells to cisplatin through PI3K/AKT/mTOR signaling pathway. *J BUON*. 2019;24:739–45.
  49. Li F, Xie W, Fang Y, Xie K, Liu W, Hou L, et al. HnRNP-F promotes the proliferation of bladder cancer cells mediated by PI3K/AKT/FOXO1. *J Cancer*. 2021;12:281–91.
  50. Li L, Sun Y, Zhang Y, Wang W, Ye C. Mutant huntingtin impairs pancreatic  $\beta$ -cells by recruiting IRS-2 and disturbing the PI3K/AKT/FoxO1 signaling pathway in Huntington's disease. *J Mol Neurosci*. 2021;71:2646–58.
  51. Razani E, Pourbagheri-Sigaroodi A, Safaroghli-Azar A, Zoghi A, Shanaki-Bavarsad M, Bashash D. The PI3K/Akt signaling axis in Alzheimer's disease: a valuable target to stimulate or suppress? *Cell Stress Chaperones*. 2021;26:871–87.
  52. Gao Y, Liao G, Xiang C, Yang X, Cheng X, Ou Y. Effects of phycocyanin on INS-1 pancreatic  $\beta$ -cell mediated by PI3K/Akt/FoxO1 signaling pathway. *Int J Biol Macromol*. 2016;83:185–94.
  53. Liu TY, Shi CX, Gao R, Sun HJ, Xiong XQ, Ding L, et al. Irisin inhibits hepatic gluconeogenesis and increases glycogen synthesis via the PI3K/Akt pathway in type 2 diabetic mice and hepatocytes. *Clin Sci (Lond)*. 2015;129:839–50.
  54. Yu F, Wei R, Yang J, Liu J, Yang K, Wang H, et al. FoxO1 inhibition promotes differentiation of human embryonic stem cells into insulin producing cells. *Exp Cell Res*. 2018;362:227–34.
  55. Calissi G, Lam EW, Link W. Therapeutic strategies targeting FOXO transcription factors. *Nat Rev Drug Discov*. 2021;20:21–38.
  56. Xing YQ, Li A, Yang Y, Li XX, Zhang LN, Guo HC. The regulation of FOXO1 and its role in disease progression. *Life Sci*. 2018;193:124–31.
  57. Kitamura T, Nakae J, Kitamura Y, Kido Y, Biggs WH 3rd, Wright CV, et al. The forkhead transcription factor Foxo1 links insulin signaling to Pdx1 regulation of pancreatic beta cell growth. *J Clin Invest*. 2002;110:1839–47.
  58. Tabatabaie PS, Yazdanparast R. Teucrium polium extract reverses symptoms of streptozotocin-induced diabetes in rats via rebalancing the Pdx1 and FoxO1 expressions. *Biomed Pharmacother*. 2017;93:1033–9.
  59. Liu X, Yan F, Yao H, Chang M, Qin J, Li Y, et al. Involvement of RhoA/ROCK in insulin secretion of pancreatic  $\beta$ -cells in 3D culture. *Cell Tissue Res*. 2014;358:359–69.

60. Bernard AB, Lin CC, Anseth KS. A microwell cell culture platform for the aggregation of pancreatic  $\beta$ -cells. *Tissue Eng Part C Methods*. 2012;18:583–92.
61. Nyitray CE, Chavez MG, Desai TA. Compliant 3D microenvironment improves  $\beta$ -cell cluster insulin expression through mechanosensing and  $\beta$ -catenin signaling. *Tissue Eng Part A*. 2014;20:1888–95.
62. Khavari A, Nydén M, Weitz DA, Ehrlicher AJ. Composite alginate gels for tunable cellular microenvironment mechanics. *Sci Rep*. 2016;6:30854.
63. Panhwar MH, Czerwinski F, Dabir VAS, Komaragiri Y, Fregin B, Biedenweg D, et al. High-throughput cell and spheroid mechanics in virtual fluidic channels. *Nat Commun*. 2020;11:2190.
64. Wassmer CH, Lebreton F, Bellofatto K, Bosco D, Berney T, Berishvili E. Generation of insulin-secreting organoids: a step toward engineering and transplanting the bioartificial pancreas. *Transpl Int*. 2020;33:1577–88.
65. Gattás-Asfura KM, Valdes M, Celik E, Stabler CL. Covalent layer-by-layer assembly of hyperbranched polymers on alginate microcapsules to impart stability and permselectivity. *J Mater Chem B*. 2014;2:8208–19.
66. Sakai S, Ono T, Ijima H, Kawakami K. MIN6 cells-enclosing aminopropyl-silicate membrane templated by alginate gels differences in guluronic acid content. *Int J Pharm*. 2004;270:65–73.
67. Simó G, Fernández-Fernández E, Vila-Crespo J, Ruipérez V, Rodríguez-Nogales JM. Research progress in coating techniques of alginate gel polymer for cell encapsulation. *Carbohydr Polym*. 2017;170:1–14.
68. Zhang M, Yan S, Xu X, Yu T, Guo Z, Ma M, et al. Three-dimensional cell-culture platform based on hydrogel with tunable microenvironmental properties to improve insulin-secreting function of MIN6 cells. *Biomaterials*. 2021;270:120687.

**Publisher's Note** Springer Nature remains neutral with regard to jurisdictional claims in published maps and institutional affiliations.

Springer Nature or its licensor (e.g. a society or other partner) holds exclusive rights to this article under a publishing agreement with the author(s) or other rightsholder(s); author self-archiving of the accepted manuscript version of this article is solely governed by the terms of such publishing agreement and applicable law.